Supporting Information for "Imaging Carrier Diffusion in Perovskites with a Diffractive Optic-Based Transient Absorption Microscope"

Zhenkun Guo, Ninghao Zhou, Olivia F. Williams, Jun Hu, Wei You, and Andrew M. Moran*

Department of Chemistry, University of North Carolina at Chapel Hill, Chapel Hill, NC 27599

I. SEM Image of Perovskite Film

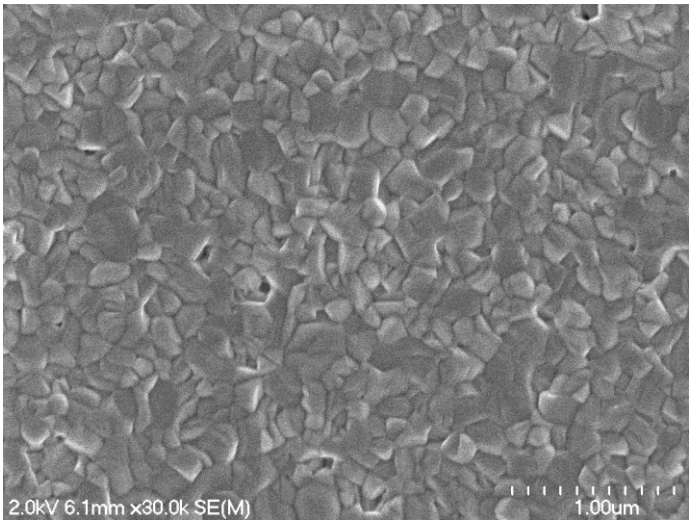

Figure S1. Individual grains are observed in this SEM image of a perovskite film.

II. SEM Image of Perovskite Single Crystal

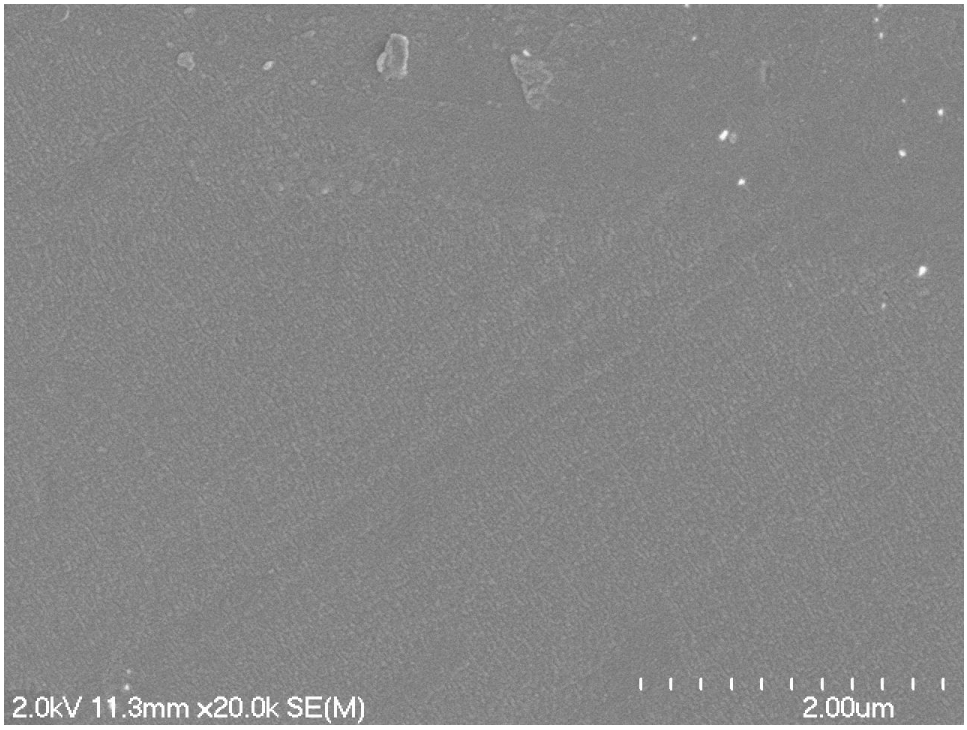

Figure S2. SEM image of perovskite single crystal.

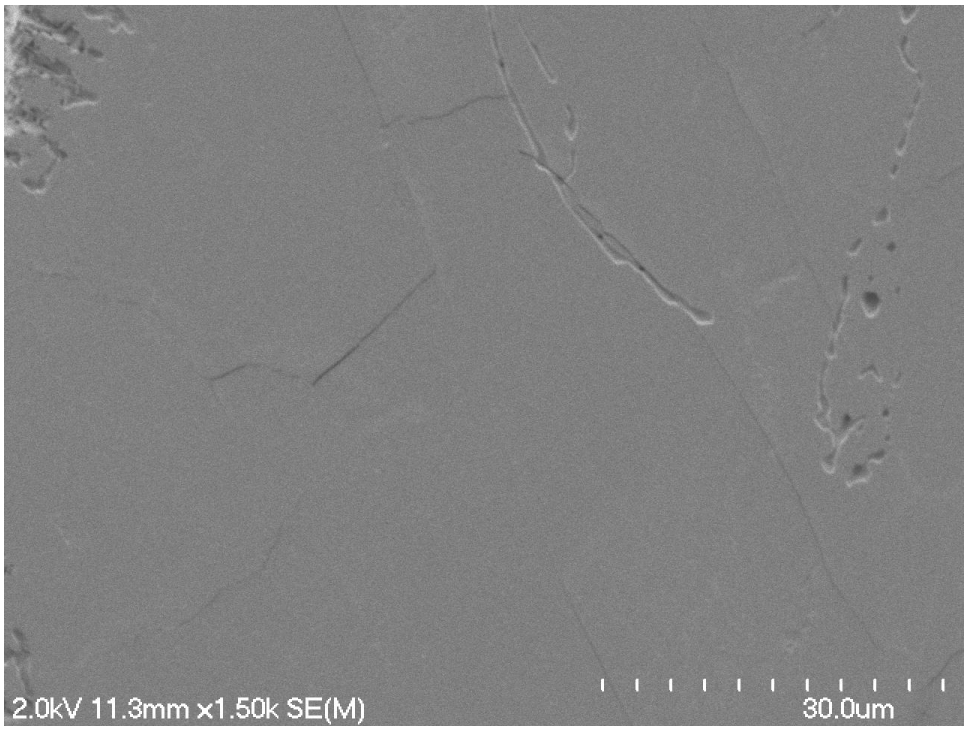

Figure S3. SEM image of perovskite single crystal.

Table S1. Carrier densities calculated at each value of the pump fluence

Fluence	Film	Crystal
27 μJ/cm^2	4.23 × 10^{18} cm^{-3}	4.52 × 10^{18} cm^{-3}
39 μJ/cm^2	6.00× 10^{18} cm^{-3}	6.41× 10^{18} cm^{-3}
50 μJ/cm^2	7.75× 10^{18} cm^{-3}	8.28× 10^{18} cm^{-3}
93 μJ/cm^2	1.44× 10^{19} cm^{-3}	1.54× 10^{19} cm^{-3}
161 μJ/cm^2	2.50× 10^{19} cm^{-3}	2.67× 10^{19} cm^{-3}
315 μJ/cm^2	4.89× 10^{19} cm^{-3}	5.22× 10^{19} cm^{-3}
905 μJ/cm^2	1.40× 10^{20} cm^{-3}	1.50× 10^{20} cm^{-3}

III. Calculating Carrier Densities

This section describes how carrier densities are calculated for the film and crystal. The carrier density is calculated by assuming Beer-Lambert absorption with the following equation,[1]

$$N = \frac{f}{h\nu l}(1 - e^{-\alpha l}) = Cf \,, \tag{S1}$$

where f is the fluence, $h\nu$ is the energy of a photon, l is the thickness of the sample and α is the absorption coefficient, which is $6.9\,\mu m^{-1}$ at 570 nm.[2] The constant, C, is determined by properties of the material. The thickness of the film is extracted from its absorption spectrum using the Beer-Lambert law,

$$l = \frac{O.D.}{\alpha}\ , \tag{S2}$$

where $O.D.$ is the optical density at 570 nm. The thickness of crystal is set equal to the inverse of the absorption coefficient (i.e., $1/e$ of the absorption length).[3] This is because the thickness of our crystal is greater than $5\mu m$, so a negligible amount of pump light can be transmitted through the sample. Therefore, the signal is predominately generated within $1/e$ of the absorption depth. Under these assumptions, the constant C is equal to $2.15\times10^{23}\,J^{-1}cm^{-1}$ for the film and $1.66\times10^{23}\,J^{-1}cm^{-1}$ for the crystal.

IV. Plots of Fitting Parameters at all Laser Spots for a Range of Fluences

The parameters determined for each pump spot and pump fluence are plotted in Figure S4 in order to illustrate variation of the dynamics for the two samples. Typically, 5-10 of the 41 beams is incident on a scattering defect on the crystal surface, which limits the number of useful spots to 33 in this experiment. The signals measured for each spot are fit with Equation (1) for both systems. The means and standard deviations are then computed to produce the summary in Figure 6 in the main article. Significant variation is found for each of the parameters. For example, the diffusion coefficients range from 0.00 to 0.10 cm^2/s in the film and from 0.04-0.36 cm^2/s in the crystal at 90 $\mu J/cm^2$. The single-body relaxation rate, τ_1^{-1}, exhibits greater variation in the crystal than it does in the film. In the crystal, the parameter, τ_1^{-1}, ranges from 0.01 to 0.46 ns^{-1} at 90 $\mu J/cm^2$. Finally, the two-body relaxation rate, τ_2^{-1}, is negligible in the crystal but significant in the film at fluences above 50 $\mu J/cm^2$. For example, the parameter, τ_2^{-1}, ranges from 0.02 to 0.80 ns^{-1} at 90 $\mu J/cm^2$ in the film.

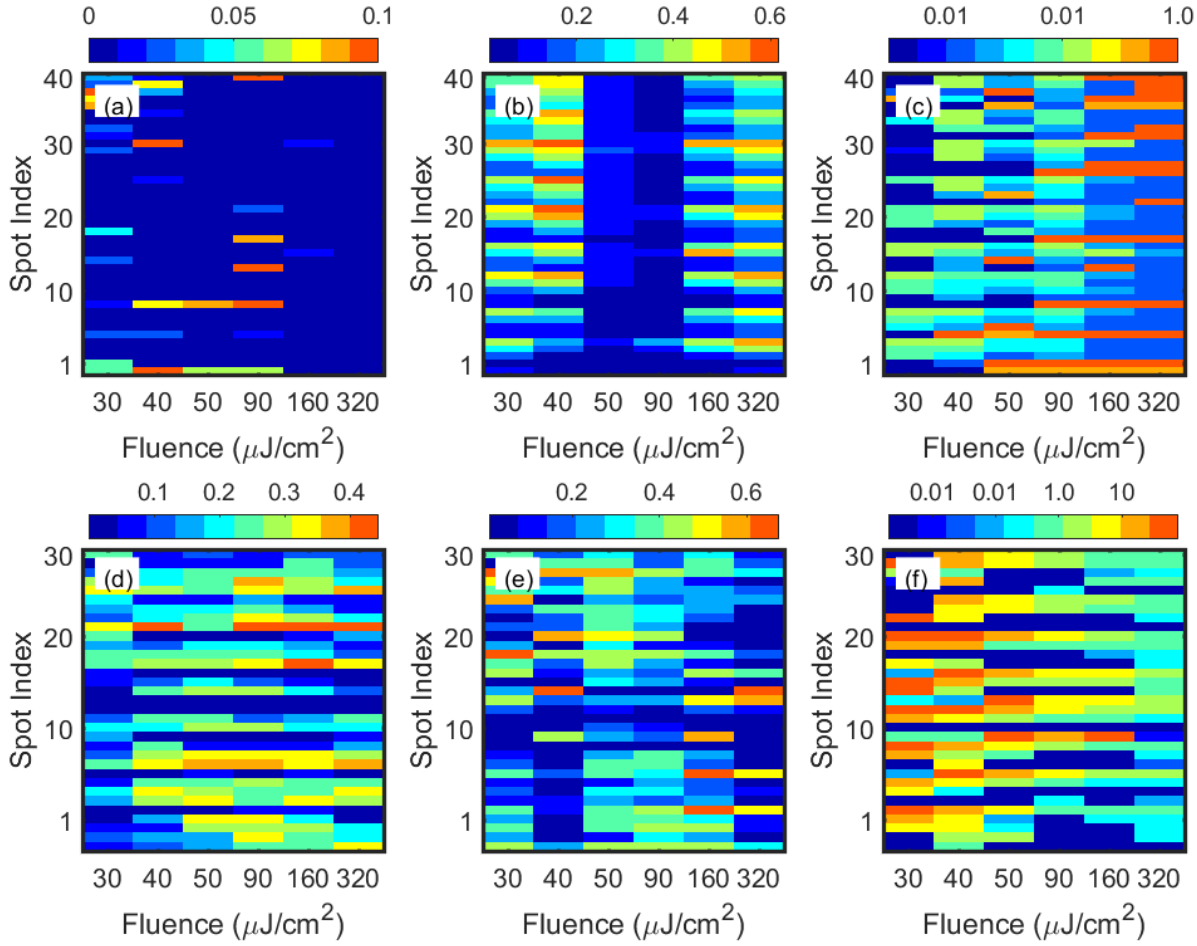

Figure S4. *Fitting parameters for all laser spots obtained for perovskite film (top) and single crystal (bottom). (a),(d) Diffusion coefficients,* D_0 *(*cm^2/s*); (b),(e) single-body relaxation rate,* τ_1^{-1} *(*ns^{-1}*); (c),(f) two-body relaxation rate,* τ_2^{-1} *(*ns^{-1}*). Averages and standard deviations for these data are shown in Figure 6 in the main article.*

Reference

1. Tian, W.; Zhao, C.; Leng, J.; Cui, R.; Jin, S. Visualizing Carrier Diffusion in Individual Single-Crystal Organolead Halide Perovskite Nanowires and Nanoplates. *J. Am. Chem. Soc.* **2015,** *137*, 12458-12461.
2. Xing, G.; Mathews, N.; Sun, S.; Lim, S. S.; Lam, Y. M.; Gratzel, M.; Mhaisalkar, S.; Sum, T. C. Long-range balanced electron- and hole-transport lengths in organic-inorganic $CH_3NH_3PbI_3$. *Science* **2013,** *342*, 344-347.

3. Hill, A. H.; Smyser, K. E.; Kennedy, C. L.; Massaro, E. S.; Grumstrup, E. M. Screened Charge Carrier Transport in Methylammonium Lead Iodide Perovskite Thin Films. *J. Phys. Chem. Lett.* **2017,** *8,* 948-953.